This is the accepted manuscript made available via CHORUS. The article has been published as:

Gravitational anomaly in the ferrimagnetic topological Weyl semimetal NdAlSi

Pardeep Kumar Tanwar, Mujeeb Ahmad, Md Shahin Alam, Xiaohan Yao, Fazel Tafti, and Marcin Matusiak

Phys. Rev. B **108**, L161106 — Published 20 October 2023

DOI: 10.1103/PhysRevB.108.L161106

Gravitational anomaly in ferrimagnetic topological Weyl semimetal NdAlSi

Pardeep Kumar Tanwar [1], Mujeeb Ahmad [1], Md Shahin Alam [1], Xiaohan Yao [2], Fazel Tafti [2] and Marcin Matusiak [1,3*]

1. *International Research Centre MagTop, Institute of Physics, Polish Academy of Sciences, Aleja Lotnikow 32/46, PL-02668 Warsaw, Poland*
2. *Department of Physics, Boston College, Chestnut Hill, Massachusetts, 02467, USA*
3. *Institute of Low Temperature and Structure Research, Polish Academy of Sciences, ul. Okólna 2, 50-422 Wrocław, Poland*

Quantum anomalies are the breakdowns of classical conservation laws that occur in quantum–field theory description of a physical system. They appear in relativistic field theories of chiral fermions and are expected to lead to anomalous transport properties in Weyl semimetals. This includes a chiral anomaly, which is a violation of the chiral current conservation that takes place when a Weyl semimetal is subjected to parallel electric and magnetic fields. A charge pumping between Weyl points of opposite chirality causes the chiral magnetic effect that has been extensively studied with electrical transport. On the other hand, if the thermal gradient, instead of the electrical field, is applied along the magnetic field, then as a consequence of the gravitational (also called the thermal chiral) anomaly an energy pumping occurs within a pair of Weyl cones. As a result, this is expected to generate anomalous heat current contributing to the thermal conductivity. We report an increase of both the magneto-electric and magneto-thermal conductivities in semi-classical regime of the magnetic Weyl semimetal NdAlSi. Our work also shows that the anomalous electric and heat currents, which occur due to the chiral magnetic effect and gravitational anomalies respectively, are still linked by a 170 years old relation called the Wiedemann-Franz law.

Corresponding author, email: *matusiak@magtop.ifpan.edu.pl

Introduction

Topological materials are a class of compounds having non-trivial electronic band structures [1-3]. Their characteristic linear energy dispersion and spin momentum locking lead to the emergence of new phenomena with potential applications in the field of spintronics and ultra-fast electronics devices [4]. Anomalous properties of topological materials have been extensively studied to date, and a list of investigated phenomena includes the chiral magnetic effect (CME) [5,6], anomalous Hall [7-10] and anomalous thermal Hall effects [11-13], chiral zero sound [14-16], mixed axial-gravitational anomaly [17-22] and more [22,23]. Some theoretical predictions have been well evidenced experimentally, some would benefit from alternative confirmation. Among the latter is the occurrence of the chiral anomaly in Weyl semimetals, which is expected to generate additional electric current, when electric and magnetic fields are parallel to each other [24-29]. This should contribute to the total electrical conductivity, hence an observation of the negative longitudinal magnetoresistance (NLMR) was initially taken as the smoking-gun evidence of the chiral anomaly [30,31]. However, it was later realised that the phenomenon could be also attributed to other factors, such as the current jetting effect [32-34] or the geometric-dependent magnetoresistance [35]. On the other hand, a charge pumping between Weyl nodes of opposite chirality is not the only anomalous behaviour of Weyl semimetals. Namely, in presence of a thermal gradient an energy pumping between Weyl nodes should also affect the entropy current and contribute both to the thermal conductivity [36] and the thermoelectric power [20,29,37]. These phenomena are supposed to be more robust to experimental artefacts [20-22,36]. Interestingly, the resulting anomalous thermal effect is recognized to be a solid-state realisation of the gravitational anomaly known from high-energy physics [19,20,22,38].

In this work, we show evidence for the presence of the gravitational anomaly in the semi-classical regime of type II magnetic Weyl semimetal NdAlSi. Previously, an increase of

the thermal conductivity with magnetic field was only observed in the extreme quantum limit of $Bi_{1-x}Sb_x$, which a particular case of a field-induced "ideal" Weyl semimetal with the Fermi level matching exactly to the position of the Weyl points [36]. We measured the thermal and electrical transport in the magnetic field parallel to the thermal gradient (or electric field), and we observed an increase in the thermal (or electrical) conductivity, indicating the emergence of the chiral thermal (or electric) current. A relation between the thermal and electrical response remains consistent with theoretical predictions. Our study shows that the gravitational anomaly can be detected in a semi-classical regime with the Fermi level not matching exactly the position of Weyl nodes.

Results and discussion

NdAlSi is a magnetic type II Weyl semimetal in which both inversion and time-reversal symmetries are broken [39-42]. Its ground state is ordered ferrimagnetically, which, with increasing temperature, transforms into an antiferromagnetic order and eventually into a high temperature paramagnetic phases [39,40]. In each state, the electronic structure of NdAlSi hosts Weyl fermions with 26, 28 and 20 pairs of Weyl nodes in the ferrimagnetic, antiferromagnetic and paramagnetic phases, respectively [39,41]. A sizable Dzyaloshinkii – Moriya interaction between local magnetic moments leads to their helical magnetic structure [39,40,42,43]. Since the incommensurate wavevector connects different non-trivial Fermi pockets, the magnetism in NdAlSi appears to be mediated by Weyl fermions [40].

Figure 1a presents the magnetic field dependences of the electrical resistivity for NdAlSi measured at various temperatures with B parallel to both the electric current and the a-axis. At low temperatures there are visible anomalies in $\rho(B)$ (like at $B \approx 2$, 10 T at $T \approx 4.7$ K, and $B \approx 12$ T at $T = 1.8$, 2.8 K), which presumably in high magnetic field marks a suppression of the spin density, as it closes the gap in the nested parts of the Fermi surface. The measurements were performed in increasing and decreasing magnetic field and we did

not notice hysteretic effects in this field region. Inset in Fig. 1a shows the zero-field temperature dependence of the resistivity with the electric current applied along the *a*-axis. From room temperature, $\rho(T)$ gradually decreases down to T_{incom} = 7.2 K, where it exhibits a kink corresponding to the paramagnetic – incommensurate spin density wave transition [39]. The incommensurate ordering wavevector decreases with decreasing temperature and at $T_{com} \approx 3.2$ K NdAlSi undergoes a transition to the commensurate chiral ferrimagnetic phase marked by another kink in $\rho(T)$ [39]. The increase of ρ below $T \approx 5.5$ K may be due to a superzone gap formation that can develop in a case when the periodicity of antiferromagnetic order is different from that of the lattice [44-46]. The transitions temperatures found here are consistent with previous reports [39,40].

For all temperatures $\rho(B)$ increases with B in the low field region, which can be due to the positive orbital longitudinal magnetoresistance (σ_0) and/or the weak antilocalization (WAL) effect [47,48]. The former can be related to Fermi surface anisotropy or the momentum – dependent scattering time [49,50]. The presence of the latter is one of the transport signatures for Weyl semimetals [47,51-54] which could be related to quantum interference of Weyl fermions [53]. The 3D WAL is expected to contribute to the total magneto-electrical conductivity (σ_{total}) as $-\sqrt{B}$ or $-B^2$, depending on the strength of the magnetic field [53]. The $\sigma_{total}(B)$ can then be quantified phenomenologically as [54]:

$$\sigma_{total}(B) = \sigma_{ch} - C_{WAL}\left(\sqrt{B}\frac{B^2}{B^2+B_C^2} + \gamma B^2 \frac{B_C^2}{B^2+B_C^2}\right) + \sigma_0, \quad (1)$$

where σ_{ch} is the anomalous chiral contribution, C_{WAL} and γ are parameters describing WAL, B_C characterises a crossover from $-\sqrt{B}$ to $-B^2$ regime ($B_c \approx \frac{\hbar}{e l_\varphi{}^2}$; $\hbar$, l_φ are the reduced Planck constant and dephasing length, respectively). The positive $\sigma_{total}(B)$ present at high temperature is unlikely due to WAL, indicating that σ_0 in NdAlSi is also field dependent. The exact form of $\sigma_0(B)$ is unknown, which makes difficult to separate the low-field positive

magnetoresistance for specific contributions. Alternatively, in the high field and for temperatures lower than $T \approx 35$ K we observe the negative longitudinal magnetoresistance (NLMR), i.e. $\rho(B)$ exhibits a negative slope. It is unlikely related to domain walls as an application of a magnetic field of just over 1 mT causes the average area of stable domains in sister Weyl semimetal CeAlSi to more than double [55] and NLMR appears in the magnetic field about four orders of magnitude higher. Moreover, the effect is also present in the paramagnetic phase.

A decrease in the resistivity only when a magnetic field is applied parallel to the electrical current and along the separation of Weyl points is referred to as the chiral magnetic effect. This macroscopic manifestation of the chiral anomaly has been reported in the number of topological semimetals and is a consequence of an imbalance in the number of Weyl fermions populating Weyl nodes of opposite chirality that leads to anomalous electric current [5,28,30,37,54,56]. The resulting additional contribution to the longitudinal electrical conductivity in semi-classical regime and for $\mu >> T$ is:

$$\sigma_{ch} = N_W \frac{e^2}{8\pi^2\hbar} \frac{(eB)^2 v^3}{\mathcal{E}_F^2} \tau_{WP} \,, \tag{2}$$

where $N_W, e, v, \mathcal{E}_F, \tau_{WP}$ are: number of Weyl nodes pairs, elementary charge, Fermi velocity, Fermi energy, and inter-valley Weyl relaxation time, respectively [57]. The latter, τ_{WP}, determines the time scale at which quasiparticles scatter between the Weyl points and change their chirality. The increase of σ should be then proportional to B^2, which is indeed the observed behaviour (both below and above T_{incom}) along with a small oscillatory component in the data presented in Fig. 1b. The frequency of these small oscillations is about 53 T (for more details, see Fig. S3 [60]) close to the β frequency (66 T), dominating the high field Shubnikov – de Haas effect for $B \parallel c$ [40]. Using the Onsager relation $A = \pi k_F^2 = 2\pi eF/\hbar$ [58] (where A is the area of the Fermi surface extreme cross-section, k_F is the Fermi wavevector, and F is the oscillations frequency), effective mass resulting from the Lifshitz-Kosevich

formula (see inset in Fig. S3): $m^* = 0.11\, m_0$ (m_0 is the free electron mass) and mobility $\mu \approx 0.1$ m^2/Vs [40] we estimated τ_{WP} (Eq. 2) and the transport relaxation time $\tau_{tr} = \frac{\mu m^*}{e}$ for $T = 10$ K. As expected for the chiral regime, the resulting $\tau_{WP} \approx 10^{-11}$ s turns out to be significantly longer that $\tau_{tr} \approx 10^{-14}$ s, which is a necessary condition for observing CME [25].

However, the chiral magnetic effect is not the only possible origin of NLMR [33-36]. This can be also caused by extrinsic effects likely occurring in materials with ultra-high mobile charge carriers [32-34], but the mobility in NdAlSi is rather moderate, which makes this material less prone to extrinsic effects [59]. Nevertheless, the ultimate confirmation of the intrinsic nature of NLMR will be an observation of a counterpart phenomenon in the heat transport, which is robust to the current jetting effect [19,20,22,38].

Figure 2 presents the temperature dependence of the thermal conductivity (κ) along with the electronic thermal conductivity estimated using Wiedemann – Franz (WF) law: $\kappa_{WF} = \sigma L_0 T$, where L_0 is the Sommerfeld value of Lorenz number for free electrons ($\kappa(T)$ dependences measured at B = 0, 5, 10 and 14.5 T are presented in Fig. S1 in Supplemental Material [60]). A maximum of $\kappa(T)$ at $T \approx 60$ K is most likely related to the lattice thermal conductivity and marks the temperature, at which Umklapp processes start to effectively disturb the phonon transport [61]. Below $T \approx 60$ K both $\kappa(T)$ and $\kappa_{WF}(T)$ decrease down to $T \approx 10$ K and at this temperature the electronic contribution appears to account for a significant portion of the total thermal conductivity. Below $T \approx 10$ K $\kappa(T)$ starts to deviate upwards and reaches a maximum at $T \approx 5$ K, which indicate that in this region magnons also participate in the heat transport. Inset in Fig. 2 shows the $\kappa(T)$ - $\kappa_{WF}(T)$ data plotted along with the estimated phonon contribution of thermal conductivity, $\kappa_l(T)$. The latter was estimated using the low-temperature constant-pressure specific heat (C_p) data of non-magnetic reference material LaAlSi, which were fitted with the function $C_p(T) = \gamma T + aT^3$, to separate the specific heat for the electronic (γT) and lattice (aT^3) contributions. Subsequently, the electronic

contribution was subtracted from $C_p(T)$ and the remaining lattice specific heat, $C_l(T)$, was scaled to match the $\kappa(T)$ - $\kappa_{WF}(T)$ of NdAlSi in the 18 – 23 K temperature range. If the phonon mean-free path (l) is constant below $T \approx 23$ K, then the resulting curve should roughly account for $\kappa_l(T)$, because $\kappa_l = 1/3\ C_v\ v_s\ l$ and we can assume that in this temperature range the speed of sound (v_s) does not change significantly and the constant-volume specific heat $C_v \approx C_p$. A low temperature extrapolation of the $\kappa_l(T)$ dependence thus obtained, shows that in this region κ_l is much smaller than total thermal conductivity, while the maximum in $\kappa(T)$ at $T \approx 5$ K comes from the magnonic contribution to the thermal conductivity (κ_m) of NdAlSi mentioned earlier.

An important question to address is to what extent the Wiedeman-Franz law can be used to calculate the electronic thermal conductivity of NdAlSi based on its electrical conductivity. In general, the WF law is valid for a Fermi liquid, as long as collisions of charge carriers can be described as elastic, which means that the heat and charge currents are affected equivalently [60]. Hence, the WF law is usually well obeyed in the high and low temperature limits. Figure 3 presents the magnetic field dependences of κ and κ_{WF} for two exemplary temperatures within the paramagnetic phase of NdAlSi. Apparently, at room temperature $\kappa_{WF}(B)$ well accounts for the field variation of the $\kappa(B)$, if a contribution from field-independent phonon thermal conductivity, $\kappa_l(300\ \text{K}) = 12.65\ \text{W m}^{-1}\ \text{K}^{-1}$, is taken into account. However, the same cannot be said for $\kappa_{WF}(20\ \text{K})$, which increases in the high field limit, whereas $\kappa(B)$ at this temperature decreases monotonically in the entire field range. A likely explanation for this discrepancy lies in no longer field-independent phonon contribution. The phonons transport is often assumed to be not affected by a magnetic field, but this is not always the case. Interestingly, there are even examples of the phonon-based thermal Hall effect occurring in non-conductive materials [62,63]. In NdAlSi, the field-dependent phonon thermal conductivity originates likely from field dependent phonon scattering efficiency and

we point at two possible underlying origins: an anharmonic phonon-phonon scattering [64] and phonon scattering on the paramagnetic free spins [65]. In the former, phonon induces the diamagnetic moment on atoms, which affects the orbital motion of valence band electrons. This phonon-induced diamagnetic moment alters the interatomic forces and leads to the magnetic-field-sensitive bond anharmonicities affecting the phonon-phonon interactions [64]. In the latter, the field sensitivity of phonon scattering is related to in-field splitting of the ground state of paramagnetic free moment Nd^{+3}. The lifting of its degeneracy leads to the two-level Schottky anomaly detected in the specific heat data [39]. The scattering of a phonon takes place in such a way that firstly, a phonon with energy equal to the energy difference between the split levels is absorbed, which excites free spin from the lower-energy state to the higher-energy. Later, another phonon is emitted by the excited state of free spin, which has the same energy but with a different wave vector.

Figure 4 presents a comparison of the magnetic field dependences of the total thermal conductivity $\kappa(B)$ to the respective $\kappa_{WF}(B)$ for several different temperatures in the low–T region. The characteristic feature of $\kappa(B)$ is its initial steep decrease, which we attribute to the suppression of the magnonic component that is expected in the noninteracting approach to decrease approximately exponentially in the magnetic field [66,67]. The dependences of the thermal conductivity on the magnetic field after subtracting $\kappa_{WF}(B)$ do indeed exhibit such a behaviour and $\kappa_m(B)$ obtained in this way can be well fitted with the exponential decay function e^{-cB} (see Fig. S2 [60]). Inset in Fig. 4 shows that for T = 5 and 6.1 K, a sum of $\kappa_{WF}(B)$ and the exponentially decaying magnonic conductivity matches very well the experimental $\kappa(B)$ data. This also indicates that magnons do not participate in thermal transport in high magnetic field limit [67,68].

Remarkably, below $T \sim 8$ K and in the high field regime, where the phonon and magnon contributions to the thermal conductivities are negligible, both $\kappa(B)$ and $\kappa_{WF}(B)$

consistently increase in a very good agreement with the Wiedemann-Franz law. At temperatures $T = 8$ K and 10 K, $\kappa_{WF}(B)$ eventually rises in the high field limit over $\kappa(B)$, which is likely due to a downward deviation of the Lorenz number below the Sommerfeld value. This is an expected consequence of the increase in temperature and the resulting difference in effectiveness of dissipation processes affecting heat and charge currents observed previously in metals and also topological semimetals [69,70]. An increasing role of inelastic scattering at high temperatures can also cause the positive thermal conductivity to be more difficult to observe. However, at low temperatures, where we expect a recovery of dominance of the elastic scattering, the high-field agreement between $\kappa(B)$ and $\kappa_{WF}(B)$ is almost perfect.

A Weyl system, which is subjected to the parallel magnetic and electric field, is expected to generate the additional electric current due to imbalance in number of Weyl fermions of opposite chirality [2,3,5,21]. On the other hand, if the thermal gradient is applied instead of the electrical field to such a material, there appears an imbalance in energy between two Weyl points of opposite chirality. The energy pumping that occurs between them leads to generation of the anomalous heat current [20,21,22,36], which results in increase of the thermal conductivity with the magnetic field. The effect stems from the gravitational anomaly appearing when chiral electrons propagate through curved space-time [17,19,22,71,72]. This violates separate conservation of energy-momentum tensor in a chiral system [21] and such a violation can be translated to thermal transport coefficients [19,20,22,72]. Astonishingly, the chiral heat current is related to the chiral electrical current by the Wiedemann-Franz law in the same way as the thermal and electric conductivities of free electrons [22,36,57]:

$$\kappa_{ch} = \frac{\pi^2 k_B^2 \sigma_{ch} T}{3e^2} = L_0 \sigma_{ch} T \tag{2}$$

Where $L_0 = \pi^2 k_B^2 / 3e^2$, k_B is the Boltzmann constant and e is the elementary charge. In other words, a Weyl semimetal is not only expected to exhibit in-field increase of the thermal

and electrical conductivities due to presence of the chiral anomaly, but these two transport coefficients should also obey the Wiedemann – Franz law. This is what we report to happen at low temperatures and high magnetic field in NdAlSi.

In summary, we have investigated the magneto-electrical and magneto-thermal transport in the antiferromagnetic Weyl semimetal NdAlSi. At low temperatures, we observed both positive magneto-electric and magneto-thermal conductivities, which appear to be related in the manner predicted by the Wiedemann – Franz law. This is the behaviour expected when additional electric and thermal currents contributions result from the quantum anomalies. The detected presence of the gravitational (or thermal chiral) anomaly in NdAlSi is a good confirmation of unusual quantum - based properties of Weyl semimetals.

Methods

Single crystals of NdAlSi were grown by a self-flux technique, details of which were described in the previous reports [39]. NdAlSi crystallizes in a non-centrosymmetric centred tetragonal structure, $I4_1md$ (C_{4v}), but in case of site mixing between Al and Si, the space group could change from non-centrosymmetric to centrosymmetric. A neutron diffraction study was used to show that such a site mixing does not occur in NdAlSi [39].

For the transport measurements, a rectangular bar with dimensions 1.9 x 1.4 x 0.35 mm^3 was cut from a suitable single crystal with the longest side of the sample oriented along the [1 0 0] direction (crystallographic *a*-axis that is a magnetic hard axis) and the shortest side along the [0 0 1] direction (crystallographic *c*-axis that is an easy axis). The electrical resistivity (ρ) was measured using a four-point technique with an alternating electric current flowing along *a*. The current contacts were made on the cross-section surface rather than point-like to maintain the homogeneous current and minimize extrinsic effects. The experiments were performed in the temperature (*T*) range 1.8 - 300 K and in the magnetic field (*B*) up to 14.5 T applied parallel to the electric current ($B \parallel a$).

The isolated heater method was used for the thermal conductivity (κ) measurements, it was described in details in [16]. During measurements the thermal gradient (∇T) was applied along *a*-axis of the single crystal NdAlSi, whereas the magnetic field was parallel to the thermal gradient. For field sweeps, a DC technique was used and up and down sweeps of the magnetic field were performed to extract the field-symmetric component of the signal. For temperature ramps at constant field the quasi-AC mode was used.

Acknowledgments

This work was supported by the Foundation for Polish Science through the IRA Programme co-financed by EU within SG OP. The material is based upon work supported by the Air Force Office of Scientific Research under award number FA2386-21-1-4059. We thank Andrzej Szewczyk, Francisco Pena Benitez and Jakub Polaczyński for insightful discussions.

Competing financial interests:

The authors declare no competing financial interests.

Data availability

All of the relevant data that support the findings of this study are available from the corresponding author upon reasonable request.

M.Matusiak ORCID iD: 0000-0003-4480-9373

References:

[1] Ling Lu, Zhiyu Wang, Dexin Ye, Lixin Ran, Liang Fu, John D. Joannopoulos, and Marin Soljacic, Experimental observation of Weyl points, *Science* **349**, 613 (2015). DOI: 10.1126/science.aaa9273

[2] Shuang Jia, Su-Yang Xu, and M. Zahid Hasan, Weyl semimetals, Fermi arcs and chiral anomalies. *Nat. mater.* **15**, 1140 (2016). DOI: https: //doi.org/10.1038/nmat4787

[3] Binghai Yan and Claudia Felser, Topological materials: Weyl semimetals. *Annu. Rev. Condens. Matter Phys.* **8**, 337 (2017). DOI: https://doi.org/10.1146/annurev-conmatphys-031016-025458

[4] Sasikanth Manipatruni, Dmitri E. Nikonov, and Ian A. Young, Beyond CMOS computing with spin and polarization, *Nat. Phys.* **14**, 338 (2018). DOI: https://doi.org/10.1038/s41567-018-0101-4

[5] N.P. Ong, and Sihang Liang, Experimental signatures of the chiral anomaly in Dirac–Weyl semimetals. *Nat. Rev. Phys.* **3**, 394 (2021). DOI: https://doi.org/10.1038/s42254-021-00310-9

[6] Qiang Li and Dmitri E. Kharzeev. Chiral magnetic effect in condensed matter systems. *Nucl. Phys. A* **956**, 107 (2016). DOI: https://doi.org/10.1016/j.nuclphysa.2016.03.055

[7] A.A. Burkov, Anomalous Hall effect in Weyl metals, *Phys. Rev. Lett.* **113**, 187202 (2014). DOI: https://doi.org/10.1103/PhysRevLett.113.187202

[8] Peigang Li, Jahyun Koo, Wei Ning, Jinguo Li, Leixin Miao, Lujin Min, Yanglin Zhu, Yu Wang, Nasim Alem, Chao-Xing Liu, Zhiqiang Mao and Binghai Yan, Giant room temperature anomalous Hall effect and tunable topology in a ferromagnetic topological semimetal Co_2MnAl, *Nat. Commun.* **11**, 3476 (2020). DOI: https://doi.org/10.1038/s41467-020-17174-9

[9] Chandra Shekhar, Nitesh Kumar, V Grinenko, Sanjay Singh, R. Sarkar, .H Luetkens, Shu-Chun Wu, Yang Zhang, Alexander C. Komarek, Erik Kampert, Yurii Skourski, Jochen Wosnitza, Walter Schnelle, Alix McCollam, Uli Zeitler, Jürgen Kübler, Binghai Yan, H.-H. Klauss, S.S.P. Parkin, and C. Felser, Anomalous Hall effect in weyl semimetal half-Heusler compounds RPtBi (R = Gd and Nd), *PNAS* **115**, 37 (2018). DOI: https://doi.org/10.1073/pnas.1810842115

[10] Md Shahin Alam, Amar Fakhredine, Mujeeb Ahmad, PK Tanwar, Hung- Yu Yang, Fazel Tafti, Giuseppe Cuono, Rajibul Islam, Bahadur Singh, Artem Lynnyk, Carmine Autieri, and Marcin Matusiak, Sign change of anomalous Hall effect and anomalous Nernst effect in the Weyl semimetal CeAlSi, *Phys. Rev. B* **107**, 085102 (2023). DOI: https://doi.org/10.1103/PhysRevB.107.085102

[11] Yago Ferreiros, A.A. Zyuzin, and Jens H. Bardarson, Anomalous Nernst and thermal Hall effects in tilted Weyl semimetals, *Phys. Rev. B* **96**, 115202 (2017). DOI: https://doi.org/10.1103/PhysRevB.96.115202

[12] Abhirup Roy Karmakar, S. Nandy, A. Taraphder, and G.P. Das, Giant anomalous thermal Hall effect in tilted type-I magnetic weyl semimetal $Co_3Sn_2S_2$, *Phys. Rev. B* **106**, 245133 (2022). DOI: https://doi.org/10.1103/PhysRevB.106.245133

[13] Chuanchang Zeng, Snehasish Nandy, and Sumanta Tewari, Chiral anomaly induced nonlinear Nernst and thermal Hall effects in Weyl semimetals, *Phys. Rev. B* **105**, 125131 (2022). DOI: https://doi.org/10.1103/PhysRevB.105.125131

[14] Zhida Song and Xi Dai, Hear the sound of Weyl fermions, *Phys. Rev. X* **9**, 021053, 2019. DOI: https://doi.org/10.1103/PhysRevX.9.021053

[15] Junsen Xiang, Sile Hu, Zhida Song, Meng Lv, Jiahao Zhang, Lingxiao Zhao, Wei Li, Ziyu Chen, Shuai Zhang, Jian-Tao Wang, Yi-feng Yang, Xi Dai, Frank Steglich, Genfu Chen, and Peijie Sun, Giant magnetic quantum oscillations in the thermal conductivity of TaAs: indications of chiral zero sound. *Phys. Rev. X* **9**, 031036 (2019). DOI: https://doi.org/10.1103/PhysRevX.9.031036

[16] Pardeep Kumar Tanwar, Md Shahin Alam, Mujeeb Ahmad, Dariusz Kac- zorowski, and Marcin Matusiak, Severe violation of the wiedemann- franz law in quantum oscillations of NbP, *Phys. Rev. B* **106**, L041106 (2022). DOI: https://doi.org/10.1103/PhysRevB.106.L041106

[17] Tohru Eguchi and Peter G.O. Freund, Quantum gravity and world topology, *Phys. Rev. Lett.* **37**, 1251 (1976). DOI: https://doi.org/10.1103/PhysRevLett.37.1251.

[18] Reinhold A. Bertlmann, Anomalies in Quantum Field Theory, Oxford, 2000; online edn, Oxford Academic (2010), DOI: https://doi.org/10.1093/acprof:oso/9780198507628.001.0001

[19]Karl Landsteiner, Eugenio Megias, and Francisco Pena-Benitez. Gravitational anomaly and transport phenomena, *Phys. Rev. Lett.* **107**, 021601 (2011). DOI: https://doi.org/10.1103/PhysRevLett.107.021601

[20] Johannes Gooth, Anna C. Niemann, Tobias Meng, Adolfo G Grushin, Karl Landsteiner, Bernd Gotsmann, Fabian Menges, Marcus Schmidt, Chandra Shekhar, Vicky Süß, Ruben Hühne, Bernd Rellinghaus, Claudia Felser, Binghai Yan and Kornelius Nielsch, Experimental signatures of the mixed axial–gravitational anomaly in the Weyl semimetal NbP, *Nature*, **547**, 324 (2017). DOI: https://doi.org/10.1038/nature23005

[21] Claudia Felser and Johannes Gooth, Topology and chirality, *ArXiv preprint, arXiv*:**2205**.05809 (2022). DOI: https://doi.org/10.48550/arXiv.2205.05809

[22] Maxim N. Chernodub, Yago Ferreiros, Adolfo G. Grushin, Karl Landsteiner, and Maria A.H. Vozmediano, Thermal transport, geometry, and anomalies, *Phys. Rep.* **977**, 1 (2022). DOI: https://doi.org/10.1016/j.physrep.2022.06.002

[23] Naoto Nagaosa, Takahiro Morimoto, and Yoshinori Tokura, Transport, magnetic and optical properties of Weyl materials, *Nat. Rev. Mat.* **5**, 621 (2020). DOI: https://doi.org/10.1038/s41578-020-0208-y

[24] Holger Bech Nielsen and Masao Ninomiya, The Adler-Bell-Jackiw anomaly and Weyl fermions in a crystal, *Phys. Lett. B*, **130**, 389 (1983). DOI: https://doi.org/10.1016/0370-2693(83)91529-0

[25] D.T. Son and B.Z. Spivak, Chiral anomaly and classical negative magnetoresistance of Weyl metals, *Phys. Rev. B* **88**, 104412 (2013).DOI: https://doi.org/10.1103/PhysRevB.88.104412

[26] Jun Xiong, Satya K Kushwaha, Tian Liang, Jason W Krizan, Max Hirschberger, Wudi Wang, Robert Joseph Cava, and Nai Phuan Ong, Evidence for the chiral anomaly in the Dirac semimetal Na_3Bi, *Science* **350**, 6259 (2015). DOI: https://doi.org/10.1126/science.aac6089

[27] Shuo-Ying Yang, Jonathan Noky, Jacob Gayles, Fasil Kidane Dejene, Yan Sun, Mathias Dorr, Yurii Skourski, Claudia Felser, Mazhar Nawaz Ali, Enke Liu, and Stuart S. P. Parkin, Field-modulated anomalous hall conductivity and planar hall effect in $Co_3Sn_2S_2$ nanoflakes, *Nano Lett.* **20**, 7860 (2020). DOI: https://doi.org/10.1021/acs.nanolett.0c02219

[28] N.P. Armitage, E.J. Mele, and Ashvin Vishwanath, Weyl and Dirac semimetals in three-dimensional solids, *Rev. Mod. Phys.* **90**, 015001 (2018). DOI: https://doi.org/10.1103/RevModPhys.90.015001

[29] Max Hirschberger, Satya Kushwaha, Zhijun Wang, Quinn Gibson, Sihang Liang, Carina A Belvin, Bogdan Andrei Bernevig, Robert J Cava, and Nai Phuan Ong, The chiral anomaly and thermopower of Weyl fermions in the half-Heusler GdPtBi, *Nat. Mat.* **15**, 1161 (2016). DOI: https://doi.org/10.1038/nmat4684

[30] Zhen Wang, Yi Zheng, Zhixuan Shen, Yunhao Lu, Hanyan Fang, Feng Sheng, Yi Zhou, Xiaojun Yang, Yupeng Li, Chunmu Feng, and Zhu-An Xu, Helicity-protected ultrahigh mobility Weyl fermions in NbP *Phys. Rev. B* **93**, 121112(R) (2016). DOI: https://doi.org/10.1103/PhysRevB.93.121112

[31] Jian Hua Du, HangDong Wang, Qianhui Mao, Rajwali Khan, Binjie Xu, Yuxing Zhou, Yannan Zhang, Jinhu Yang, Bin Chen, Chunmu Feng, and Ming Hu Fang, Large unsaturated positive and

negative magnetoresistance in Weyl semimetal TaP, *Sci. China Phys. Mech. Astron*. **59**, 657406 (2016). DOI: https://doi.org/10.1007/s11433-016-5798-4

[32] Frank Arnold, Chandra Shekhar, Shu-Chun Wu, Yan Sun, Ricardo Donizeth Dos Reis, Nitesh Kumar, Marcel Naumann, Mukkattu O. Ajeesh, Marcus Schmidt, Adolfo G. Grushin, Jens H. Bardarson, Michael Baenitz, Dmitry Sokolov, Horst Borrmann, Michael Nicklas, Claudia Felser, Elena Hassinger and Binghai Yan, Negative magnetoresistance without well-defined chirality in the Weyl semimetal TaP, *Nat. Comm.* **7**, 11615 (2016). DOI: https://doi.org/10.1038/ncomms11615

[33] R.D. Dos Reis, M.O. Ajeesh, N. Kumar, F. Arnold, C. Shekhar, M. Naumann, M. Schmidt, M. Nicklas, and E. Hassinger, On the search for the chiral anomaly in Weyl semimetals: the negative longitudinal magnetoresistance, *New J. Phys* **18**, 085006 (2016). DOI 10.1088/1367-2630/18/8/085006

[34] M. Naumann, F. Arnold, M. D. Bachmann, K. A. Modic, P. J. W. Moll, V. Suß, M. Schmidt, and E. Hassinger, Orbital effect and weak localization in the longitudinal magnetoresistance of Weyl semimetals NbP. NbAs, TaP, TaAs. *Phys. Rev. Mater*. **4**, 034201 (2020). DOI: https://doi.org/10.1103/PhysRevMaterials.4.034201

[35] Katsukuni Yoshida, A geometrical transport model for inhomogeneous current distribution in semimetals under high magnetic fields, *JPSJ* **40**, 1027 (1976). DOI: https://doi. org/10.1143/JPSJ.40.1027

[36] Dung Vu, Wenjuan Zhang, Cuneyt Sahin, Michael E. Flatte, Nandini Trivedi, and Joseph P Heremans, Thermal chiral anomaly in the magnetic- field-induced ideal Weyl phase of Bi_{1-x} Sb_x, *Nat. Mat.* **20**, 1525 (2021). DOI: https://doi.org/10.1038/s41563-021-00983-8

[37] Zhenzhao Jia, Caizhen Li, Xinqi Li, Junren Shi, Zhimin Liao, Dapeng Yu, and Xiaosong Wu, Thermoelectric signature of the chiral anomaly in Cd_3As_2. *Nat. Commun.* **7**, 13013 (2016). DOI: https://doi. org/10.1038/ncomms13013

[38] R. Loganayagam and Piotr Surówka, Anomaly/transport in an ideal Weyl gas, *JHEP* **2012**, 97 (2012). DOI: https://doi.org/10.1007/JHEP04(2012)097

[39] Jonathan Gaudet, Hung-Yu Yang, Santu Baidya, Baozhu Lu, Guangyong Xu, Yang Zhao, Jose A Rodriguez-Rivera, Christina M. Hoffmann, David E. Graf, Darius H. Torchinsky, Predrag Nikolić, David Vanderbilt, Fazel Tafti and Collin L. Broholm, Weyl-mediated helical magnetism in NdAlSi, *Nat. Mat.* **20**, 1650 (2021). DOI: https://doi.org/10.1038/s41563-021-01062-8

[40] Jin-Feng Wang, Qing-Xin Dong, Zhao-Peng Guo, Meng Lv, Yi-Fei Huang, Jun-Sen Xiang, Zhi-An Ren, Zhi-Jun Wang, Pei-Jie Sun, Gang Li, and Gen-Fu Chen, NdAlSi: A magnetic Weyl semimetal candidate with rich magnetic phases and atypical transport properties, *Phys. Rev. B* **105**, 144435 (2022). DOI: https://doi.org/10.1103/PhysRevB.105.144435

[41] Santu Baidya, David Vanderbilt, Jonathan Gaudet, Hung-Yu Yang, Fazel Tafti, and Collin Broholm, NdAlSi, a type-II magnetic Weyl semimetal, *APS March Meeting Abstracts* **2021**, P51–008, (2021). DOI: https://meetings.aps.org/Meeting/MAR21/Session/P51.8.

[42] Jin-Feng Wang, Qing-xin Dong, Yi-Fei Huang, Zhao-Sheng Wang, Zhao- Peng Guo, Zhi-Jun Wang, Zhi-An Ren, Gang Li, Pei-Jie Sun, Xi Dai, Gen-Fu Chen, Temperature dependent quantum oscillations at a constant magnetic field in a magnetic Weyl semimetal, *ArXiv preprint, arXiv*:**2201**.06412 (2022). DOI: https://doi.org/10.48550/arXiv.2201.06412

[43] Predrag Nikolić, Dynamics of local magnetic moments induced by itinerant Weyl electrons, *Phys. Rev. B* **103**, 155151 (2021). DOI: https://doi.org/10.1103/PhysRevB.103.155151

[44] I. Das and R. Rawat, A study of magnetocaloric effect in $PrCo_2Si_2$ to understand contributions to magnetoresistance, *Solid State Commun.* **115**, 207 (2000). DOI: https://doi.org/10.1016/S0038-1098(00) 00165-4

[45] A.R. Mackintosh, Magnetic ordering and the electronic structure of rare-earth metals, *Phys. Rev. Lett.* **9**, 90 (1962). DOI: https://doi.org/10.1103/PhysRevLett.9.90

[46] Hirosi Miwa, Energy gaps and electrical resistivity associated with screw- type spin arrangements, *Prog. Theor. Phys.* **29**, 477 (1963). DOI: https://doi.org/10.1143/PTP.29.477

[47] Xiaochun Huang, Lingxiao Zhao, Yujia Long, Peipei Wang, Dong Chen, Zhanhai Yang, Hui Liang, Mianqi Xue, Hongming Weng, Zhong Fang, Xi Dai, and Genfu Chen, Observation of the chiral-anomaly-induced negative magnetoresistance in 3d Weyl semimetal TaAs, *Phys. Rev. X* **5**, 031023 (2015). DOI: https://doi.org/10.1103/PhysRevX.5.031023

[48] Jin-Hyeon Jun, Jinsu Kim, Sang Hyun Ji, Sang-Eon Lee, Soo-Whan Kim, Sung Jung Joo, Kyoung-Min Kim, Ki-Seok Kim, and Myung-Hwa Jung, Negative magnetoresistance in antiferromagnetic topological insulating phase of $Gd_xBi_{2-x}Te_{3-y}Se_y$, *APL Materials* **11**, 021106 (2023). DOI: https://doi.org/10.1063/5.0135811

[49] H.K. Pal and D.L. Maslov, Necessary and sufficient condition for longitudinal magnetoresistance, *Phys. Rev. B* **81**, 214438 (2010).DOI: https://doi.org/10.1103/PhysRevB.81.214438

[50] E.H. Sondheimer, The Boltzmann equation for anisotropic metals, *Proc. R. Soc. Lond. Ser. A* **268**, 100 (1962). DOI: https://doi.org/10.1098/ rspa.1962.0128

[51] Shinobu Hikami, Anatoly I. Larkin, and Yosuke Nagaoka, Spin-orbit interaction and magnetoresistance in the two dimensional random system, *Prog. Theor. Phys.* **63**, 707 (1980). DOI: https://doi.org/10.1143/PTP.63.707

[52] Heon-Jung Kim, Ki-Seok Kim, J.-F. Wang, M. Sasaki, N. Satoh, A. Ohnishi, M. Kitaura, M. Yang, and L. Li. Dirac versus Weyl fermions in topological insulators: Adler-Bell-Jackiw anomaly in transport phenomena, *Phys. Rev.. Lett.* **111**, 246603 (2013). DOI: https://doi.org/10.1103/PhysRevLett.111.246603

[53] Hai-Zhou Lu and Shun-Qing Shen, Weak antilocalization and localization in disordered and interacting Weyl semimetals, *Phys. Rev. B* **92**, 035203 (2015). DOI: https://doi.org/10.1103/PhysRevB.92.035203

[54] Cheng-Long Zhang, Su-Yang Xu, Ilya Belopolski, Zhujun Yuan, Ziquan Lin, Bingbing Tong, Guang Bian, Nasser Alidoust, Chi-Cheng Lee, Shin- Ming Huang, Tay-Rong Chang, Guoqing Chang, Chuang-Han Hsu, Horng-Tay Jeng, Madhab Neupane, Daniel S. Sanchez, Hao Zheng, Junfeng Wang, Hsin Lin, Chi Zhang, Hai-Zhou Lu, Shun-Qing Shen, Titus Neupert, M. Zahid Hasan and Shuang Jia, Signatures of the Adler–Bell–Jackiw chiral anomaly in a Weyl fermion semimetal, *Nat. Commun.* **7**, 10735 (2016). DOI: https://doi.org/10.1038/ncomms10735

[55] B. Xu, J. Franklin, A. Jayakody, H.-Y. Yang, F. Tafti, I. Sochnikov, Picoscale Magnetoelasticity Governs Heterogeneous Magnetic Domains in a Noncentrosymmetric Ferromagnetic Weyl Semimetal, *Adv. Quantum Tech.* **4**, 2000101 (2021). DOI: https://doi.org/10.1002/qute.202000101

[56] M. Kanagaraj, Jiai Ning, and Liang He, Topological $Co_3Sn_2S_2$ magnetic Weyl semimetal: from fundamental understanding to diverse fields of study, *Rev. Phys.* **8**, 100072 (2022). DOI: https://doi.org/10.1016/j.revip.2022.100072

[57] B.Z. Spivak and A.V. Andreev, Magnetotransport phenomena related to the chiral anomaly in Weyl semimetals, *Phys. Rev. B* **93**, 085107 (2016). DOI: https://doi.org/10.1103/PhysRevB.93.085107

[58] David Shoenberg, Magnetic oscillations in metals, *Cambridge University Press* (1984).

[59] Alfred Brian Pippard. Magnetoresistance in metals (Cambridge Studies in Low Temperature Physics, Series Number 2), *Cambridge University Press* (2009).

[60] See Supplemental Material at [URL will be inserted by publisher] for data on the temperature dependences of the thermal conductivity measured in zero-field and for B = 5, 10, 14.5 T applied

along the a-axis; fitting of magnetic field dependence of non-electronic thermal conductivity; evolution of the quantum oscillations with temperature; and data on the transverse magnetoresistance.

[61] John M. Ziman, Electrons and phonons: the theory of transport phenomena in solids, *Oxford university press* (1960).

[62] C. Strohm, G.L.J.A. Rikken, and P. Wyder. Phenomenological evidence for the phonon Hall effect, *Phys. Rev. Lett.* **95**, 155901 (2005). DOI: https://doi.org/10.1103/PhysRevLett.95.155901

[63] Xiaokang Li, Benoit Fauque, Zengwei Zhu, and Kamran Behnia. Phonon thermal Hall effect in strontium titanate, *Phys. Rev. Lett.* **124**, 105901 (2020). DOI: https://doi.org/10.1103/PhysRevLett.124.105901

[64] Hyungyu Jin, Oscar D. Restrepo, Nikolas Antolin, Stephen R. Boona, Wolfgang Windl, Roberto C. Myers, and Joseph P. Heremans. Phonon-induced diamagnetic force and its effect on the lattice thermal conductivity, *Nat. Mat.* **14**, 601 (2015). DOI: https://doi.org/10.1038/nmat4247

[65] X.F. Sun, I. Tsukada, T. Suzuki, Seiki Komiya, and Yoichi Ando, Large magnetothermal effect and spin-phonon coupling in a parent insulating cuprate $Pr_{1.3}La_{0.7}CuO_4$, *Phys. Rev. B* **72**, 104501 (2005). DOI: https://doi.org/10.1103/PhysRevB.72.104501

[66] D. Walton, J.E. Rives, and Q. Khalid, Thermal transport by coupled magnons and phonons in yttrium iron garnet at low temperatures, *Phys. Rev. B* **8**, 1210 (1973). DOI: https://doi.org/10.1103/PhysRevB.8.1210

[67] R.L. Douglass. Heat transport by spin waves in yttrium iron garnet. *Phys. Rev.* **129**, 1132 (1963). DOI: https://doi.org/10.1103/PhysRev.129.1132

[68] D.J. Sanders and D. Walton, Effect of magnon-phonon thermal relaxation on heat transport by magnons, *Phys. Rev. B* **15**, 71489 (1977). DOI: https://doi.org/10.1103/PhysRevB.15.1489

[69] G.K. White and R.J. Tainsh, Lorenz number for high-purity copper, *Phys. Rev.* **119**, 1869 (1960). DOI: https://doi.org/10.1103/PhysRev.119.18699

[70] Alexandre Jaoui, Benoit Fauque, Carl Willem Rischau, Alaska Subedi, Chenguang Fu, Johannes Gooth, Nitesh Kumar, Vicky Suß, Dmitrii L Maslov, Claudia Felser and Kamran Behnia, Departure from the Wiedemann–Franz law in WP_2 driven by mismatch in t-square resistivity prefactors, *Npj Quantum Mater.* **3**, 64 (2018). DOI: https://doi.org/10.1038/s41535-018-0136-x

[71] Luis Alvarez-Gaume and Edward Witten, Gravitational anomalies, *Nucl. Phys. B* **234**, 269 (1984). DOI: https://doi.org/10.1016/0550-3213(84)90066-X

[72] Karl Landsteiner, Notes on anomaly induced transport, *Acta Phys. Pol. B* **47**, 2617 (2016). DOI: https://doi.org/10.5506/APhysPolB.47.261

Figures

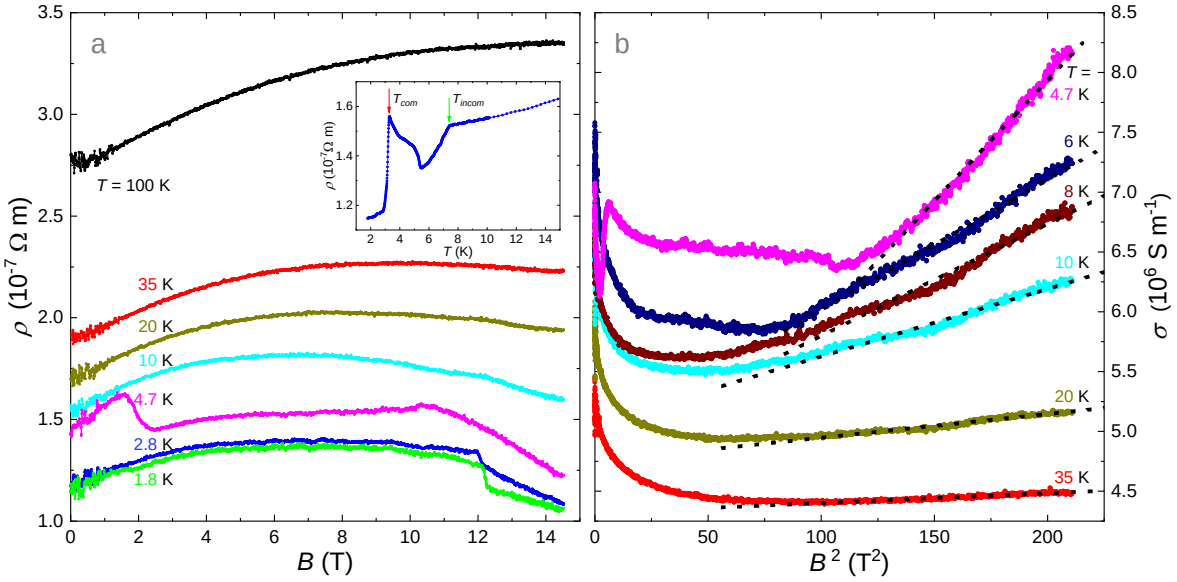


Figure 1. Magnetic field dependences of the electrical resistivity and conductivity of NdAlSi measured with the electric current and magnetic field parallel to each other and oriented along *a*-axis. Panel (a) presents $\rho(B)$ plots for several different temperatures. Inset in this panel shows the zero-field temperature dependence of the resistivity measured along [100] with anomalies at T_{incom} = 7.2 K (green arrow) and T_{com} = 3.2 K (red arrow) marking the incommensurate antiferromagnetic to commensurate ferromagnetic and paramagnetic to incommensurate antiferromagnetic transitions, respectively. Panel (b) presents Positive magneto-thermal conductivity plotted versus square of the magnetic field, where the dashed lines shows B^2 behaviour in the high field limit.

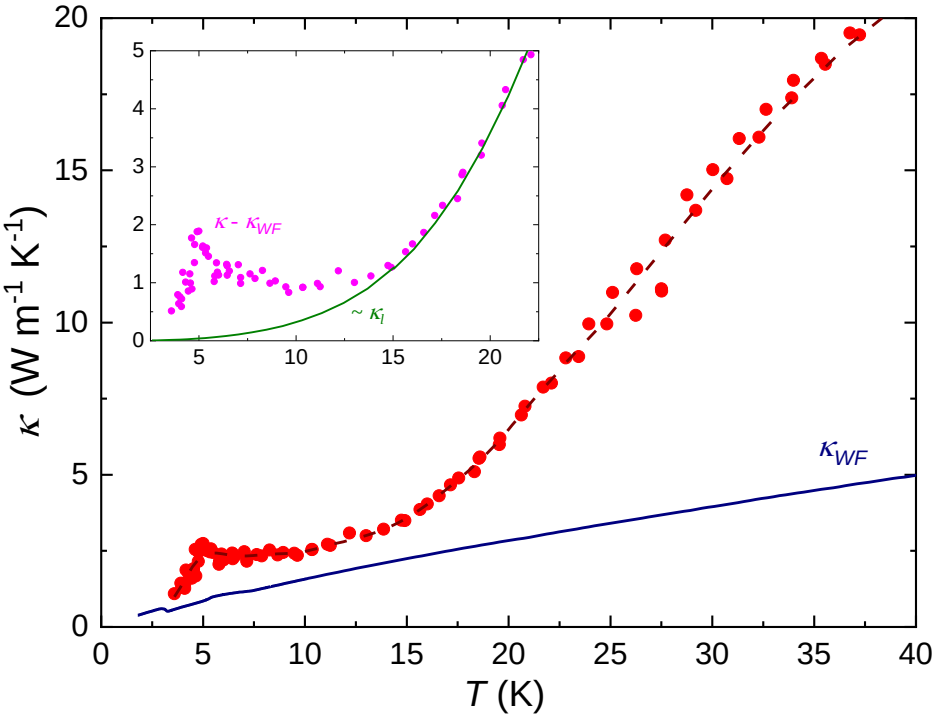


Figure 2. The temperature dependence of the *a*-axis thermal conductivity for NdAlSi in zero magnetic field. $\kappa(T)$ data is plotted with red points along with the electronic contribution $\kappa_{WF}(T)$ (dark blue line) calculated using the Wiedemann-Franz law. The dark red dashed line is a guide for the eye. Inset shows temperature dependence of the difference ($\kappa - \kappa_{WF}$) and phonon contribution to thermal conductivity $\kappa_l(T)$ (solid-green line) estimated using the LaAlSi specific heat data.

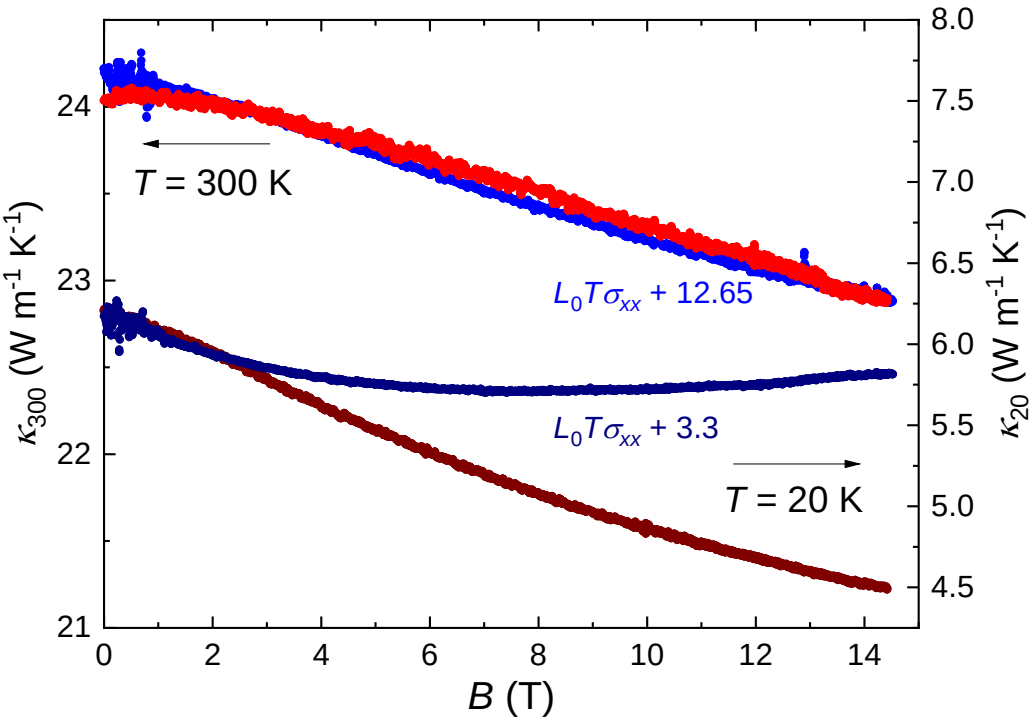


Figure 3. The Wiedemann – Franz law. The magnetic field dependences of the thermal conductivity $\kappa(B)$ for NdAlSi at T = 20 and 300 K (plotted in dark red and red, respectively). These are compared with the corresponding $\kappa_{WF}(B)$ to which a presumably field independent phonon contribution has been added.

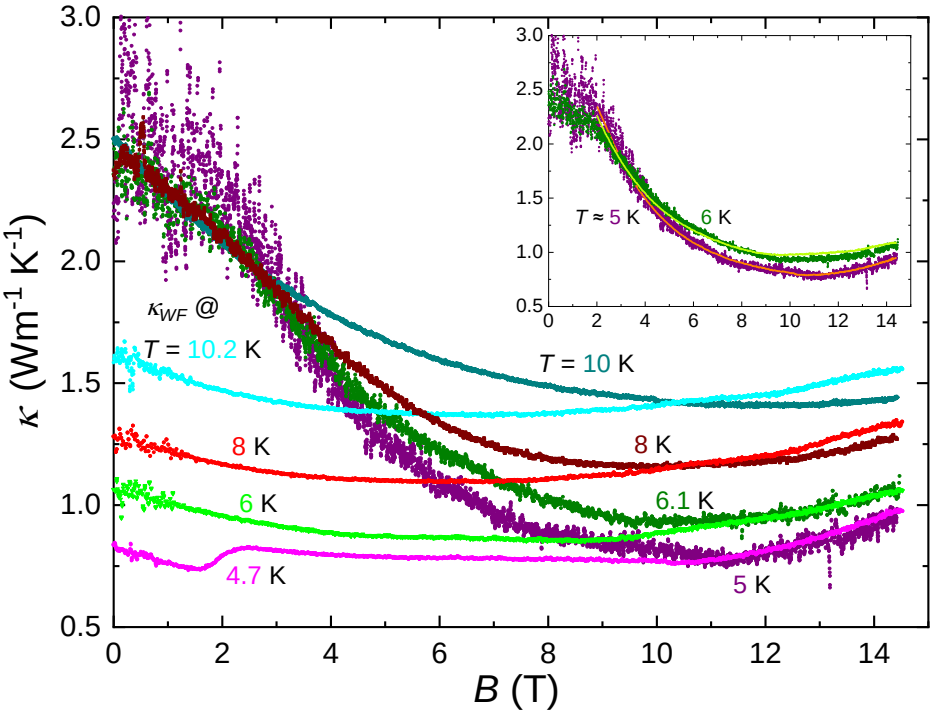


Figure 4. Increase in the thermal conductivity of NdAlSi in the low temperature and high field range. Dependences of the thermal conductivity on magnetic field compared to the corresponding $\kappa_{WF}(B)$. Inset shows $\kappa(B)$ at $T \approx 5$ and 6 K (purple and dark green, respectively) plotted with $\kappa_{WF}(B) + \kappa_m(B)$ (pink and green for $T \approx 5$ and 6 K, respectively), where $\kappa_m(B)$ is assumed to decay exponentially in the magnetic field (see Fig. S2 in SI).